

## SPEED CONTROL OF A PV POWERED DC MOTOR DRIVING A SELF-EXCITED 3-PHASE INDUCTION GENERATOR FOR MAXIMUM UTILIZATION EFFICIENCY

S. M. Alghuwainem

E.E. Department, King Saud University  
Riyadh, Saudi Arabia 11421

### Abstract

Photovoltaic (PV) powered dc motors driving dedicated loads (e.g. water pumps) are increasingly used in the remote rural areas of many developing countries. The key to their success is simplicity (direct coupling, no dc-ac conversion, no storage batteries, etc.). Because of the relatively high cost of the PV array, the system designer is interested in maximizing its utilization efficiency. A PV powered dc motor can also be used to drive a three-phase self-excited induction generator (SEIG). This arrangement is useful as part of an integrated renewable energy system (IRES), which takes advantage of the inherent diversity of wind and solar energy in most developing countries to improve power quality. The SEIG is driven by a wind-turbine, dc motor, or both. Another advantage of this arrangement is its versatile control characteristics through the dc motor control. This paper describes a technique to maximize the utilization efficiency of the PV array by controlling the field current of the dc motor through a dc chopper.

**Keywords:** - Photovoltaic generators; solar cells; dc motors; induction generators; integrated renewable energy systems.

### INTRODUCTION

Utilities in many developing countries are finding it increasingly difficult to establish and maintain remote rural area electrification. The cost of delivering power to such areas is becoming excessively high due to large investments in transmission lines, fuel transportations, locally installed generation capacities, and transmission line losses. For these reasons, many utilities are seriously considering local renewable energy resources, mainly wind and PV, as alternatives for supplying energy to rural remote areas. In many developing countries,

wind and insolation are complementary over the annual cycle [1]. It is therefore desirable to take advantage of this inherent diversity by combining PV and wind systems into one integrated renewable energy system (IRES). In addition to minimizing the overall system cost by sharing some of the equipment, the IRES improves power quality and minimizes the need for energy storage.

PV arrays convert solar energy to dc electrical power, which may be used directly by some loads where energy is stored in batteries or converted to ac power using dc-ac inverter. Inverter control equipment, peak power trackers, harmonic filters, and protection devices are all incorporated with the inverter in one unit called power conditioning unit (PCU). The cost of the PCU, efficiency, and reliability, are important factors to consider when opting for dc-ac inversion. The simplest and least expensive means to convert PV power to mechanical power is to use it directly to drive a dc motor. PV powered dc motors driving dedicated loads are increasingly used in the remote rural areas of many developing countries. The key to their success is simplicity (direct coupling, no dc-ac conversion, no storage batteries, etc.). This arrangement is typically used on noncritical loads such as water pumps, which need not operate continuously and water can be used directly or stored easily.

Due to the relatively high cost of the PV array, the system designer is interested in achieving its full utilization efficiency by matching the dc motor to the PV array. At any particular solar insolation level, there is a unique operating point on the volt-ampere characteristics of the PV array at which power output at that insolation level is maximum, possible. However, since the maximum power point varies with insolation during the day and from season to season, it is difficult to maintain maximum utilization efficiency at all insolation levels. In order to overcome this problem, the system designer may either select a compromise matching, or use an electronic control device, known as a peak-power tracker (PPT), which continuously matches the output characteristics of the PV generator to the input characteristics of the dc motor. Reference [2] is a comprehensive study of the starting and steady-state performance of several types of PV powered dc motors driving several types of water pumps. In [3], matching of dc motors to PV generators for maximum daily gross mechanical energy is reported. Peak-power tracking is achieved either by dis-

96 SM 570-2 EC A paper recommended and approved by the IEEE Energy Development and Power Generation Committee of the IEEE Power Engineering Society for presentation at the 1996 IEEE/PES Summer Meeting, July 28 - August 1, 1996, Denver, Colorado. Manuscript submitted January 4, 1996; made available for printing June 25, 1996.

cretely interchanging the series-parallel connections of solar cell modules within the PV array [4], or by using a controlled dc-dc converter to adjust the voltage and current levels [5-8].

In reference [9] a dc motor is used to drive a squirrel-cage three-phase self excited induction generator (SEIG). This arrangement is useful as part of an integrated renewable energy system (IRES), which takes advantage of the inherent diversity of wind and insolation in most developing countries [1] to improve power quality. The SEIG is driven by wind turbine, dc motor, or both. An additional advantage of this arrangement is its versatile control characteristics through the dc motor control which can be utilized to improve the system utilization efficiency. One of the major drawbacks of the isolated SEIG is that its frequency, terminal voltage, and shaft-torque vary considerably with speed and load. Therefore it is difficult to achieve a unique operating condition which maximizes utilization efficiency. This paper describes a technique to maximize utilization efficiency as the solar insolation, load, or both vary, by automatically adjusting the speed of the dc motor using a step-up dc chopper in the field circuit.

### OPERATION WITHOUT SPEED CONTROL

The motor is connected directly to the terminals of the PV generator as shown in Fig. 1.  $D_1$  is a diode to prevent reversal of current and  $D_2$  is a free-wheeling diode to provide a path for the armature current of the dc motor.

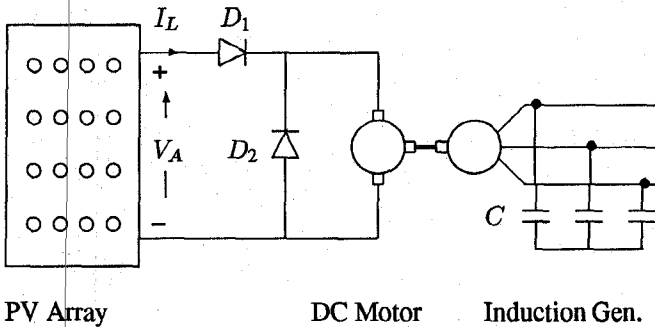


Fig. 1 Operation Without Speed Control

The system consists of three different devices; the SEIG, dc motor, and PV array. The line current of the PV array is equal to the line current of the dc motor which depends on the applied terminal voltage and speed. The speed depends on the torque requirement of the SEIG which depends on the connected load  $R_L$  and excitation capacitance  $C$ . A stable equilibrium speed exists at which the torque developed by the dc motor is equal to the torque required by the SEIG and the total system rotational losses. The common terminal voltage and current of the PV array and motor are determined by this equilibrium speed. For maximum utilization efficiency of the PV array, the equilibrium operating point must be such that current drawn by the dc motor and its terminal voltage correspond to the maximum-power-output point of the PV array.

### CHARACTERISTICS OF THE SEIG

The SEIG has been used for many years to convert wind power to electrical power. Due to its simplicity, ruggedness, and low cost, it provides a reliable and relatively inexpensive means to convert mechanical wind power to electrical power over a wide range of rotor speeds for loads where frequency and voltage need not be regulated. Over the past decade, many researchers have investigated the steady-state performance of the SEIG [10-12]. References [13-15] evaluate the excitation capacitance requirements of the SEIG under different load and speed conditions. The SEIG is actually an induction motor that is driven by a prime mover while its stator excitation is provided by an external capacitors connected to the stator. Because the SEIG is isolated, its stator frequency is free to vary with the rotor speed and the operating slip remains small and negative. Fig. 2 shows the per-phase equivalent circuit commonly used for the steady-state analysis of the three-phase self-excited induction generator [10].

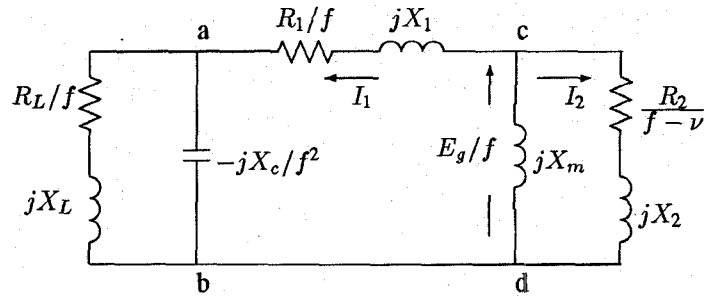


Fig. 2 Per-phase equivalent circuit of the SEIG

The circuit has been transformed to the base frequency (60 Hz) by introducing the parameters  $f$  and  $\nu$ , where  $f$  is the per-unit frequency and  $\nu$  is the per-unit speed (base speed is the synchronous speed).

The total voltage drop around the loop may be written as

$$I_1 Z_s = 0 \quad (1)$$

Therefore, for successful voltage build-up the total series impedance  $Z_s$  must be equal to zero, since  $I_1 \neq 0$ .

$$Z_{ab} + Z_{ac} + Z_{cd} = 0 \quad (2)$$

where

$$Z_{ab} = \frac{-jX_c/f^2(R_L/f + jX_L)}{R_L/f + jX_L - jX_c/f^2}$$

$$Z_{ac} = R_1/f + jX_1$$

$$Z_{cd} = \frac{jX_m(R_2/(f-\nu) + jX_2)}{R_2/(f-\nu) + jX_m + jX_2}$$

The air-gap voltage  $E_g$  is related to  $X_m$  and  $f$  through the magnetization characteristics of the machine which may be expressed as a polynomial in  $X_m$  using curve fitting:

$$\frac{E_g}{f} = a + bX_m + cX_m^2 \quad (3)$$

where  $a$ ,  $b$ , and  $c$  are known constants. Equation (2) is a non-linear equation with complex coefficients. It is normally solved by separating the real and imaginary parts to obtain two polynomial equations in  $f$  and  $X_m$ . The air-gap voltage  $E_g$  is then calculated from (3). In this paper the Mathcad [16] software which is capable of solving a system of nonlinear equations with complex coefficients is used to solve (2) and (3) for  $f$  and  $E_g$ , subject to the constraints that  $f$  and  $E_g$  are both real.

In this paper, the induction machine used is a 3-phase, 4-pole, 60 Hz, 380 V, 1.0 kW, star-connected, squirrel-cage whose per-phase equivalent circuit parameters in per unit are as follows:  $R_1 = 0.1$ ,  $X_1 = 0.2$ ,  $R_2 = 0.06$ ,  $X_2 = 0.2$ . The air-gap voltage  $E_g$  is related to the magnetizing reactance  $X_m$  by the no load magnetization characteristics which is approximated by a polynomial in  $X_m$

$$\frac{E_g}{f} = 1.12 + 0.078X_m - 0.146X_m^2 \quad 0 \leq X_m \leq 3$$

A stable operating point exists, provided that  $X_m$  is less than the unsaturated value (3 p.u.). Having determined the frequency  $f$  and the air-gap voltage  $E_g$ , the equivalent circuit of Fig. 2 is completely solved for the steady-state performance of the induction generator. The electrical torque is given by

$$T_{IG} = \frac{3|I_2|^2 R_2}{f - \nu} \quad (4)$$

where  $I_2$  is the rotor current and  $R_2$  is the rotor resistance. From the equivalent circuit, the rotor current is given by

$$I_2 = \frac{E_g/f}{R_2/(f - \nu) + jX_2} \quad (5)$$

Figs. 3 and 4 are plots of the air-gap voltage and the electrical torque variations with speed.

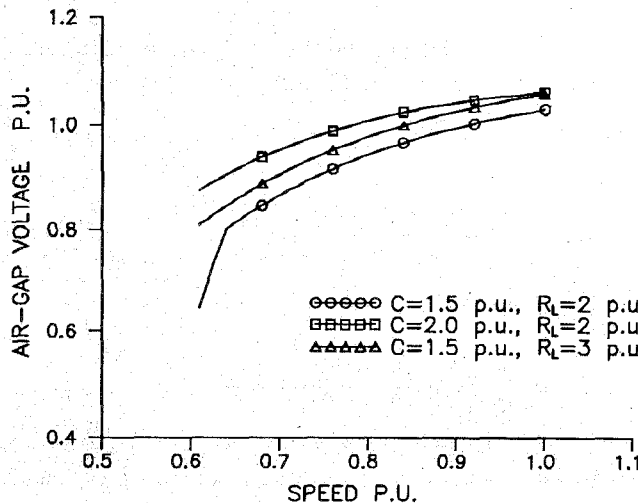


Fig. 3 SEIG's Air-Gap Voltage Variation with Speed

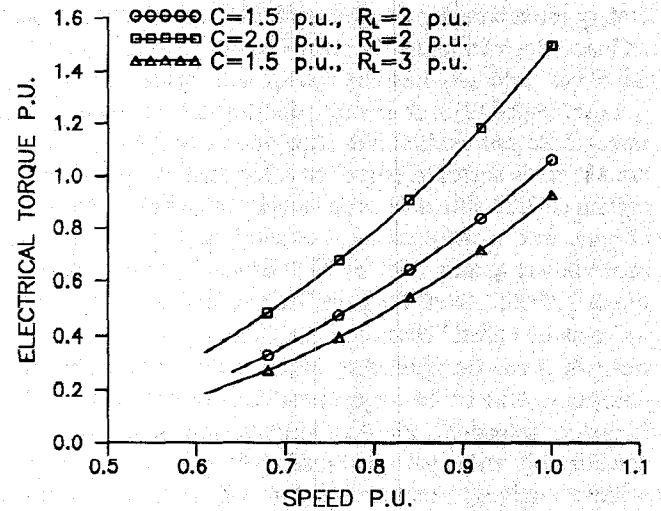


Fig. 4 SEIG's Electrical Torque Variation with Speed

## CHARACTERISTICS OF THE DC MOTOR

The dc motor used in this study is a 120V, 13.2A, 1800 r/min., having  $R_A = 1.9 \Omega$ , and  $K_a = 0.513$  H. The steady-state voltage, current, speed, and torque are related by the following equations:

$$V_A = K_a \phi \omega + R_A I_A \quad (6)$$

$$T_M = K_a \phi I_A = T_{IG} + T_{RL} \quad (7)$$

where  $T_{IG}$  is the electrical torque of the SEIG, and  $T_{RL} = 0.2 + 0.003\omega$ , is the total system rotational losses (N-M).

## CHARACTERISTICS OF THE PV ARRAY

A PV array consists of several PV modules connected in series-parallel combinations to provide the desired dc voltage and current. The overall volt-ampere characteristics of the array depend on the number of cells in series and the number of parallel strings. The PV array used in this study consists of 18 parallel strings, 324 cells in series per string, such that the overall terminal voltage  $V_L$  is given by

$$V_L = 23.68 \ln \left( \frac{I_{PH} - I_L + 0.009}{0.009} \right) - 0.9 I_L \quad (8)$$

where  $I_{PH}$  is a variable photocurrent directly proportional to the solar insolation level ( $I_{PH} = 14.4$  A., when the insolation is  $1 \text{ kW/m}^2$ ), and  $I_L$  is the load current.

Fig. 5 is a plot of the PV array I-V characteristics. The dashed line indicates the locus of the volt and current points at which power output is maximum for different solar insolation levels.

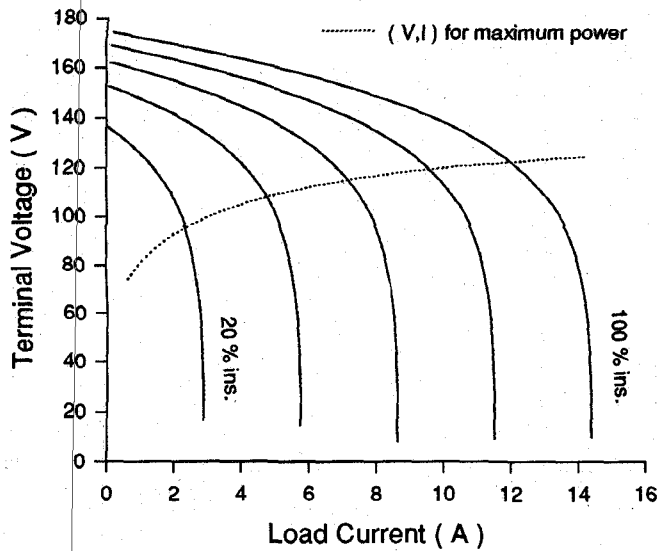


Fig. 5 V-I Characteristics of the PV Array

Since the motor terminals are connected directly to the PV array, the terminal voltage and current for both devices is the same. The common terminal voltage and current are dictated by the equilibrium speed of the dc motor which is dictated by the torque-speed characteristics of the mechanical load which is in this case the SEIG. Fig. 6 shows that the actual operating points do not coincide with the maximum power points of the PV array (the dashed line) and hence the PV array is not fully utilized.

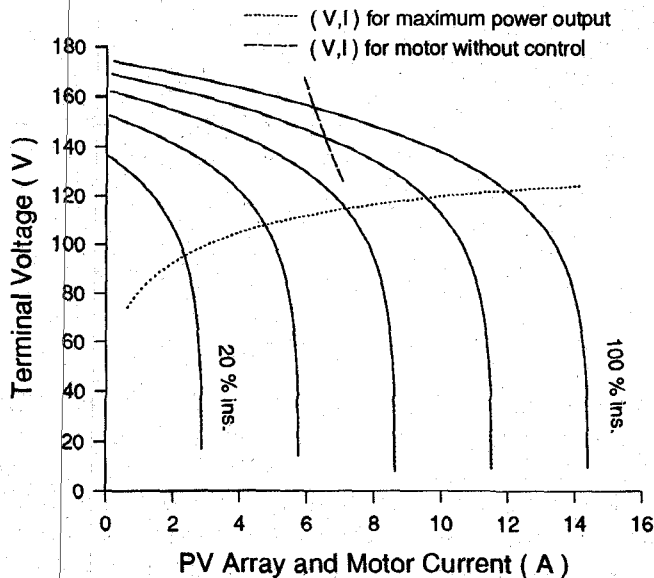


Fig. 6 V-I Characteristics of the PV Array and Motor

The technique proposed in this paper forces the motor to take more current at less voltage by reducing the speed (increasing field flux) until the motor V-I characteristics coincide with the maximum power line of the PV array. In order to shift the equilibrium operating points to coincide with the maximum power

points as the solar insolation varies it is necessary to adjust the motor current according to insolation level as described in the next section.

### CONDITION FOR MAXIMUM POWER

Voltage and current of the PV array at maximum power may be derived by first multiplying (8) by  $I_L$  to obtain the expression for power as follows:

$$P_A = 23.68 I_L \ln \left( \frac{I_{PH} - I_L + 0.009}{0.009} \right) - 0.9 I_L^2 \quad (9)$$

At maximum power

$$\frac{dP_A}{dI_L} = 0 \quad (10)$$

Therefore

$$\ln \left( \frac{I_{PH} - I_L + 0.009}{0.009} \right) - 0.076 I_L - \frac{I_L}{I_{PH} - I_L + 0.009} = 0 \quad (11)$$

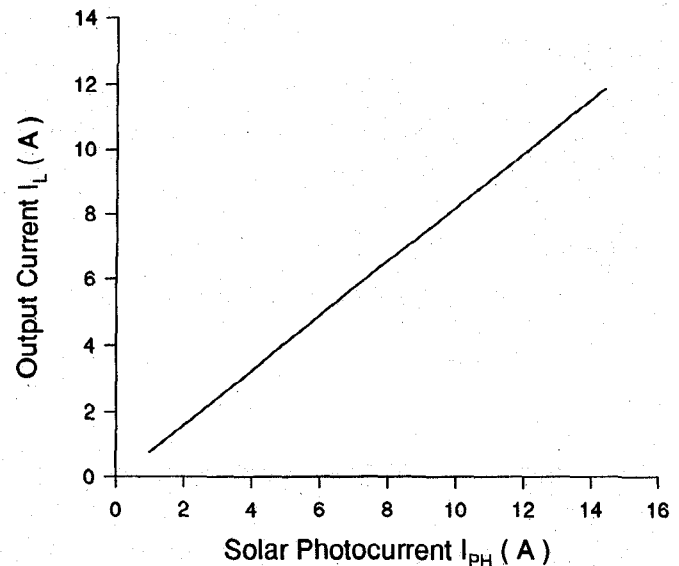


Fig. 7 Variation of Array Current with Photocurrent at Maximum Power

Fig. 7 is a plot of  $I_L$  versus  $I_{PH}$  according to equation (11) which shows a linear relationship between  $I_L$  and  $I_{PH}$  of the form

$$I_L = 0.85 I_{PH} \quad (12)$$

This linear relationship is utilized to achieve maximum power operation by controlling the speed of the dc motor through field control such that line current varies with insolation level according to (12). Two voltage signals are derived; one is proportional to  $I_L$  and the other is proportional to  $I_{PH}$ . The photocurrent  $I_{PH}$  is proportional to the short-circuit current of a cell module that is exposed to the same solar insolation level.

The difference between the two signals which is proportional to  $I_L - 0.85 I_P H$  is used as input to the driver circuit.

### THE PROPOSED TECHNIQUE

The proposed technique is based on controlling the speed of the dc motor by controlling the field current such that current drawn from the PV array corresponds to maximum power output [7,8]. The armature winding is connected directly to the PV array while the field winding is connected to the PV array through a step-up dc chopper as shown in Fig. 8. The chopper ratio is determined by the driver circuit which is basically a voltage-controlled oscillator (VCO) whose output is a periodic rectangular pulse having a duty ratio  $k$  ( $k = t_{ON}/(t_{OFF} + t_{ON})$ ) proportional to its input voltage. This pulse turns the chopper on and off by the same duty ratio.

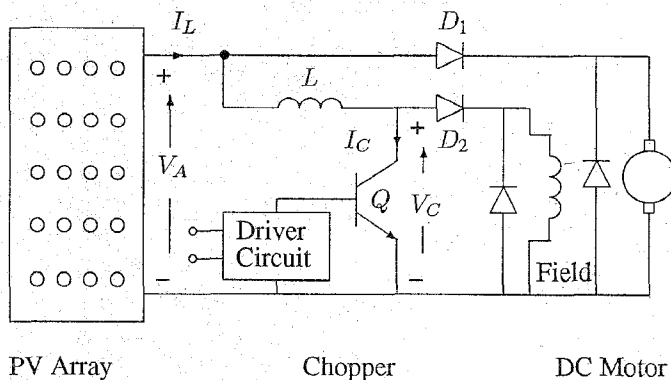


Fig. 8 Set-Up of The Proposed Technique

### OPERATION WITH SPEED CONTROL

The driver circuit controls the duty ratio of the field-circuit chopper according to the error signal. When the error voltage is different from zero the duty ratio will increase or decrease depending on the sign of the error signal until the error signal becomes zero. At low insolation levels the duty ratio  $k$  is less than one, and it increases to one at 100% insolation ( $I_{ph} = 14.4$  A). The speed increases with insolation but because of the field control, the motor current is always proportional to the solar photocurrent of the PV array in order to satisfy the maximum power output condition for maximum utilization efficiency.

Fig. 9 is a plot of the motor voltage, current and speed variations with photocurrent. In Fig. 10 the V-I characteristics of the dc motor is superimposed on the V-I characteristics of the PV array where it shows the close matching of the motor curve to the maximum power line of the PV array (the dashed line) at all insolation levels.

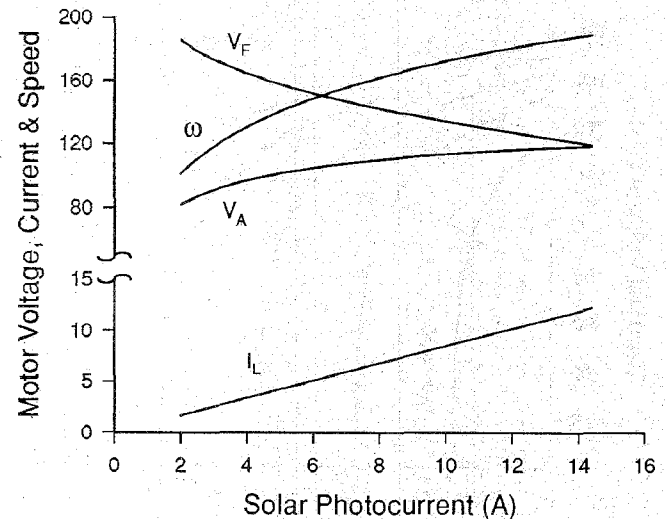


Fig. 9 Motor Voltage, Current, and Speed Variation with Photocurrent

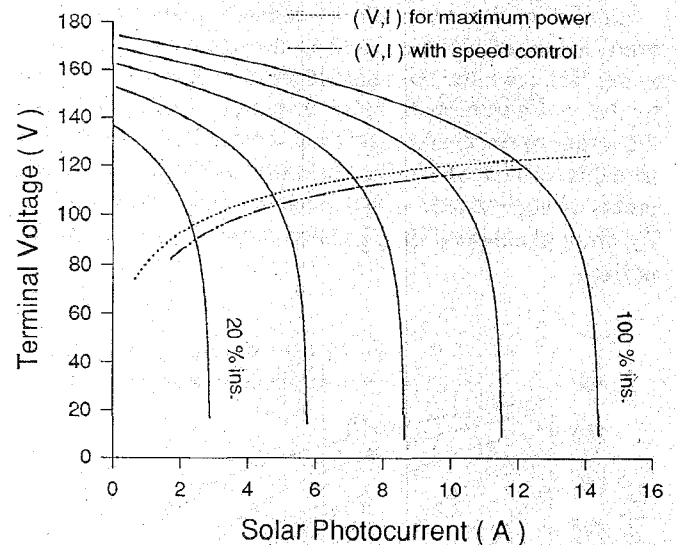


Fig. 10 Common V-I Characteristics

### CONCLUSIONS

The speed of a PV powered dc motor driving a three-phase self-excited induction generator is controlled in such a way as to achieve maximum utilization of the PV array. The armature winding of the dc motor is connected directly to the PV array, while the field winding is connected to the same PV array through a step-up dc chopper. As the solar insolation increases the voltage applied to the dc motor increases but the current drawn by the motor is kept proportional to solar insolation level by adjusting the speed to satisfy the maximum power condition. It is advantageous to control the field current rather than the armature current since the field current is much smaller than armature current and hence the chopper is less expensive. This technique eliminates the need for matching devices or peak power trackers which would add to the

cost of the system considerably. If constant frequency operation is more important than maximum utilization, the same technique can be used to control the field current to achieve constant speed (constant frequency) operation. The present arrangement with field control provides a simple, relatively inexpensive, and reliable alternative for supplying three phase power to the rural remote areas of the developing countries. It can be readily used as part of an integrated renewable energy system (IRES) in which the SEIG is driven by a wind turbine, a PV powered dc motor, or both. Since solar energy and wind energy are complementary to each other over the annual cycle in many developing countries, the IRES can be designed to take advantage of this inherent diversity to improve power quality and minimize energy storage requirements.

### REFERENCES

- [ 1 ] R. Ramakumar, "Renewable energy sources and developing countries," *IEEE Trans. Power Apparatus Syst.*, vol. PAS-102, no. 2, pp. 502-510, Feb. 1983.
- [ 2 ] J. Appelbaum, "Starting and steady-state characteristics of dc motors powered by solar cell generators," *IEEE Trans. on Energy Conversion*, vol. EC-1, no. 1, pp. 17-25, March 1986.
- [ 3 ] M. M. Saied, "Matching of dc motors to photovoltaic generators for maximum daily gross mechanical energy," *IEEE Trans. on Energy Conversion*, vol. EC-3, no. 3, pp. 465-472, September 1988.
- [ 4 ] Z. Zinger, and A. Braunstein, "Dynamic matching of a solar-electrical ( photovoltaic ) system - An estimation of the minimum requirements on the matching system," *IEEE Trans. Power Apparatus and Systems*, vol. PAS-100, no. 3, pp. 1189-1192, March 1981.
- [ 5 ] S. M. Alghuwainem, "Application of a dc chopper to maximize utilization of solar-cell generators," Paper 91 WM 145-3 EC, 1991 *IEEE/PES* 1991 Winter Meeting, New York, New York, Feb. 3-7, 1991.
- [ 6 ] M. M. Saied, A. A. Hanafy, et al., "Optimal design parameters for a PV array coupled to a dc motor via a dc-dc transformer," *IEEE Trans. on Energy Conversion*, vol. EC-6, no. 4, pp. 593-598, December 1991.
- [ 7 ] S. M. Alghuwainem, "Steady-state performance of dc motors supplied from photovoltaic generators with a step-up converter," *IEEE Trans. on Energy Conversion*, vol. EC-7, no. 2, pp. 267-272, June 1992.
- [ 8 ] S. M. Alghuwainem, "Matching of a dc motor to a photovoltaic generator using a step-up converter with a current-locked loop," *IEEE Trans. on Energy Conversion*, vol. EC-9, no. 1, pp. 192-198, March 1994.
- [ 9 ] S. M. Alghuwainem, "Performance analysis of a PV powered dc motor driving a 3-phase self-excited induction generator," *IEEE Trans. on Energy Conversion*, vol. 11, no. 1, pp. 155-161, March 1996.
- [ 10 ] S.S. Murthy, O.P. Malik, and A.K Tandon, "Analysis of self-excited induction generators," *IEE Proceedings*, vol. 129, Pt. C, no. 6, pp. 260-265, Nov. 1982.
- [ 11 ] L. Ouazene and G. McPherson, Jr., "Analysis of the isolated induction generator," *IEEE Trans. Power Apparatus Syst.*, vol. PAS-102, no. 8, pp. 2793-2798, Aug. 1983.
- [ 12 ] N.H. Malik and S.E. Hague, "Steady state analysis and performance of an isolated self-excited induction generator," *IEEE Trans. on Energy Conversion*, vol. EC-1, no. 3, pp. 134-139, Sep. 1986.
- [ 13 ] N.H. Malik and A.H. Al-Bahrani, "Influence of the terminal capacitor on the performance characteristics of a self excited induction generator," *IEE Proceedings*, vol. 137, Pt. C, no. 2, pp. 168-173, Mar. 1990.
- [ 14 ] A.K. Al Jabri and A.I. Alolah, "Limits on the performance of three-phase induction generators," *IEEE Trans. on Energy Conversion*, vol. EC-5, no. 2, pp. 350-356, June 1990.
- [ 15 ] T.F. Chan, "Capacitance requirements of self-excited induction generators," *IEEE Trans. on Energy Conversion*, vol. EC-8, no. 2, pp. 304-311, June 1993.
- [ 16 ] Mathcad User's Guide, MathSoft Inc., Cambridge, Massachusetts, 1994.



Saad M. Alghuwainem received B.Sc. in Electrical Engineering from University of Riyadh in 1974. From 1974 to 1976 he worked as a teaching assistant in the EE Department, Riyadh University. He received M.Sc. degree in Electrical Engineering from University of Colorado, Boulder in 1978. From 1979 to 1981 he worked in the EE Department, King Saud University as a research assistant.

From 1982 to 1986 he attended The University of Michigan, Ann Arbor where he received Ph.D. in Electrical Engineering. Since 1986 he has been with the Department of Electrical Engineering, King Saud University, where he is currently an associate professor. His interests include renewable energy sources, energy conversion systems, power system protection, and electromagnetic transients.